Keith M. Gawlik
National Renewable Energy Laboratory,
1617 Cole Blvd.,
Golden, CO 80401
e-mail: keith_gawlik@nrel.gov

Charles F. Kutscher
National Renewable Energy Laboratory,
1617 Cole Blvd.,
Golden, CO 80401
e-mail: chuck_kutscher@nrel.gov

Wind Heat Loss From Corrugated, Transpired Solar Collectors

Heat transfer from a perforated, sinusoidal plate with suction to air flowing over the plate, perpendicular to the corrugations, has been studied numerically and experimentally. This study used a numerical model, validated by wind tunnel tests and hot wire anemometer/resistance thermometer measurements, to determine the heat loss to the air stream over the plate as a function of wind speed, suction velocity, and plate geometry. Both attached and separated flow regimes were observed, and the criterion for flow attachment was determined to be $Re_{V0,P} \geq 6.93\, Re_{U\infty,A}^{0.5}$. *Correlations were developed for heat transfer to the air stream for each flow regime. For attached flow, the heat transfer can be represented as* $Nu_{att} = Nu_{flat}\{1 + 0.81(A/P)^{0.5}\}$. *For separated flow, the following correlation applies:* $Nu_{sep} = 2.05(A/P)^{1.40}\, Re^{1.63}$. [DOI: 10.1115/1.1487886]

Introduction

This study investigated the convective heat loss that is present when air flows over a corrugated, perforated plate with suction. Air flows over the plate perpendicular to the corrugations. This heat loss is an important term for evaluating the efficiency of transpired solar collectors that are used to heat building ventilation or process air. Such collectors are typically corrugated to provide structural stiffness. To illustrate the plate geometry and air and heat flows, Fig. 1 shows a side view of two corrugations of the plate. The test plate is warmed by short wavelength radiant heat transfer, and cooled by convective heat transfer to the suction air and to the air flowing over the surface and long wavelength radiant heat transfer to the environment. The three components of a heat balance on the plate are the heat transfer, Q_{del}, to the air drawn in through the perforations at a mean face velocity of V_0; the net radiative exchange with the environment, $Q_{rad,net}$; and the convective heat loss to the crosswind, Q_{loss}. The total convective heat loss from the plate surface to a crosswind of velocity U_∞ is the thermal energy content of the boundary layers blown off the downstream edge of the collector. The geometry of the sinusoidal corrugations is described by their amplitude, A, and pitch, P.

A characteristic of perforated plates with uniform suction at the surface and in the presence of a crosswind is the boundary layers approach a constant thickness at which the terms related to diffusion and convection to the suction air are balanced [1]. Similar behavior was observed in this study of perforated, corrugated plates in the manner described below. This is shown in Fig. 2. After the starting length, L_s, from the leading edge, the velocity and thermal boundary layer thicknesses closely approach constant average values over a corrugation. While the thicknesses may vary over a corrugation, that variation is the same for each corrugation in the asymptotic region. In the asymptotic region, all the net radiative heat flux incident on the plate is transferred to the process air as Q_{del}. All of the energy lost to the crosswind off the downstream edge of the plate was added to the crosswind along the starting length.

The problem of characterizing convective heat loss from corrugated, perforated plates with uniform suction has not been explored in the literature. Past work on perforated plates with uniform suction has focused on the flat plate geometry. Iglisch [2] investigated the flow in the developing region and determined the point at which the flow is considered asymptotic, and his work was improved by others [3]. In the asymptotic region of a flat plate, a simple exact solution of the momentum and thermal energy boundary layer equations of motion is possible and is detailed in Arpaci et al. [4]. Kutscher [5] and Kutscher et al. [6] showed how these results can be used to determine flat plate heat loss and conducted an experimental verification of the results. But the flow over a corrugated plate differs from a flat plate in a number of ways. In the case of a corrugated plate with suction, an asymptotic state is reached but it is characterized by a cyclicly repeating flow pattern over the corrugations. Also, observations made in the course of this study show that the starting length for the corrugated plate boundary layers, under the same conditions of suction and crosswind speed as for a flat plate, is greater than that for the flat plate. In addition, the boundary layer over the corrugated plate was observed to be laminar and may be fully attached or partially separated over the corrugation depending on the crosswind speed and amount of suction.

The literature on sinusoidal plates contains analyses of laminar boundary layers, but the surfaces are not perforated and do not have active, uniform suction. Bordner [7,8] wrote two papers on the nonlinear analysis of laminar boundary layers with the amplitude of the corrugations much smaller than the boundary layer thickness. The situation encountered in the present study is very different: suction is present, which thins the momentum and thermal boundary layers, and the resulting boundary layer thicknesses were found to be much smaller than the characteristic plate dimensions.

The characterization of convective heat loss from corrugated plates is not only unexplored, but is especially important for plates where the amount of convective heat loss becomes large relative to the energy delivered to the suction air. It was found in this study that corrugated plate convective heat loss can be up to 17 times greater than for a flat plate under similar conditions. Crosswind air flow perpendicular to the corrugations was studied; it was expected that flow parallel to the corrugations would be similar to flow over a flat plate.

In this study, numerical and experimental analyses were performed. The experimental apparatus did not allow tests over a wide range of suction conditions for the corrugated plate. Numerical analysis allowed a large range of flow variables and a number of plate styles to be tested. Experimental studies were employed to validate key numerical results. The correlations for convective heat loss were then developed using the numerical results.

Methodology

Numerical Modeling Approach. The commercial code, FLUENT, was used for numerical modeling. This program solves

Contributed by the Solar Energy Division of the THE AMERICAN SOCIETY OF MECHANICAL ENGINEERS for publication in the ASME JOURNAL OF SOLAR ENERGY ENGINEERING. Manuscript received by the ASME Solar Energy Division, March 2001; final revision, January 2002. Associate Editor: K. Den Braven.

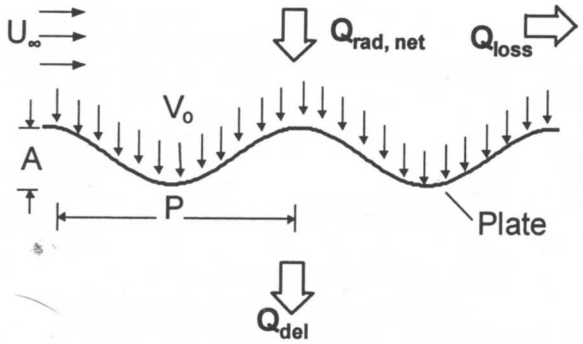

Fig. 1 Corrugated plate geometry, air flow velocity vectors, and heat flows

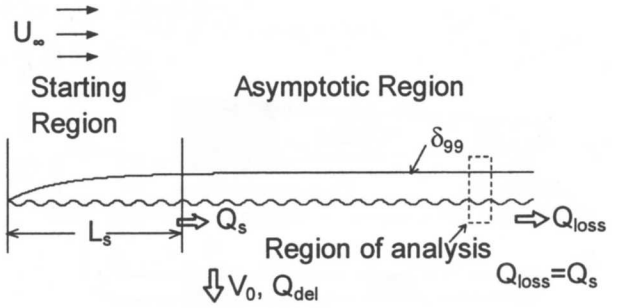

Fig. 2 Boundary layer development over plate with suction (not to scale). Net heat transfer into thermal boundary layer during starting length development is manifest as wind heat loss at the downstream end of the plate.

the full Navier-Stokes and energy conservation equations in primitive variables using the finite volume method [9]. Version 4.25 was used on Silicon Graphics workstations.

Numerical Model Description. A commercially available corrugated plate [10] was modeled as a sinusoidal plate. The commercial material was a corrugated, quasi-sinusoidal, 1% porosity aluminum plate. Crests and troughs of the quasi-sinusoid were arc segments with 0.013 m radii of curvature. The arcs were connected by straight sections. The amplitude of the corrugation was 0.0142 m, and the peak-to-peak distance was 0.0668 m. While the material was not a pure sinusoid, the sinusoid used in the numerical study closely matched the actual plate shape. By using a sinusoidal geometry, it was possible to vary the amplitude and wavelength through a simple mathematical relationship. Also, previous work in the literature often used sinusoidal geometries, so these results can be compared directly to those of others. Three aspect ratios, defined as the ratio of the wave amplitude to pitch, were modeled. The geometries are shown in Table 1.

The geometry was developed in the FLUENT preprocessor, preBFC, which allowed the use of boundary-fitted coordinates. The upstream and downstream boundaries perpendicular to the plate were cyclic to model the case of thermal and velocity boundary layers that have become asymptotic; i.e., each corrugation has the same flow and temperature fields as the previous one. The far-field boundary parallel to the plate was located sufficiently far from the plate so that its presence did not influence the boundary layers near the surface and was defined as a uniform velocity inlet. At this boundary the suction air velocity and crosswind speed were defined.

Homogeneous suction was modeled at the wall. The actual plate has 1.6 mm (0.063 in.) diameter holes arranged in a triangular pattern with 1–2% open area. A 3-D model of the plate would have required excessive computational effort to model properly, and convergence, if possible, would have taken an extremely long time. Fortunately, experimental work (see later) showed that there is an insignificant influence of the discrete holes on the 2-D boundary layer.

The flow was modeled as laminar based on experimental experience. Because of the low turbulence intensity of the airstream from the wind tunnel and the low speed of the flows over the plate, this was a reasonable assumption and was verified by smoke visualization. Laminar models yielded separated flows under common conditions of crosswind and suction speeds for the base case style plate, and this was consistent with laboratory observations under the same conditions. Simulations with turbulent flows did not show separation under these conditions. Attached flow did occur, though, in the laminar model and in the laboratory, for combinations of low crosswind speed and high suction for the base case plate.

Table 1 Plate geometries

Plate designation	Amplitude (cm)	Pitch (cm)	Aspect ratio
Base case	1.42	6.68	0.213
Low aspect-1	1.42	13.4	0.106
Low aspect-2	0.71	6.68	0.106
High aspect	1.42	3.34	0.426

The grid size depended on the plate geometry. The smallest number of cells was used for expediency in calculation, and the number of cells was increased until the heat loss calculation was insensitive to grid density. The smallest number of cells was 10,404 for the low aspect ratio plate, and the highest was 20,700 for the base case plate. Grid sensitivity studies verified that a sufficient number of cells was used in each model.

The significant parameters in the corrugated plate study were crosswind speed, suction velocity, and temperature difference between the plate and ambient. Crosswind speed and suction velocity were defined at the far-field boundary condition. Three crosswind speeds of 2, 3.5, and 5 m/s were used. The suction velocities were 0.03, 0.06, and 0.09 m/s. Temperature differences of 5, 12.5, and 20°C were used in the base case plate simulations. A 20°C temperature difference was used for the other plates. These values spanned the range of practical suction velocities and temperature differences and include typical crosswind speeds. The values of u-velocity and temperature at the crest were obtained from the simulation results and integrated to calculate the amount of heat convected in the boundary layer at the crest.

Questions that came up early in the investigation were whether the convective heat loss varied over the corrugation, and if so, whether the plate edge should be at the point in the corrugation where the convective heat loss was least. This was explored for a typical, high heat loss case with the medium aspect ratio plate. For a crosswind speed of 4 m/s, a mass flux of 0.06 kg/s-m^2, and a plate-to-air temperature difference of 12.5°C, the heat loss at the crest was 86.4 W/m. At one-quarter of the pitch distance along the plate surface, the heat loss was 85.0 W/m. At the trough, the heat loss was 81.1 W/m, and at 3/4 of the pitch distance the heat loss was 82.0 W/m. The maximum variation in heat loss over the corrugation was 5%, and this seemed too low a variation to warrant a recommendation that plates be mounted with the troughs at the edges. Also, using the crest heat losses would yield a conservative correlation for convective heat loss.

Qualification Tests using Experimental Results. Experimental runs were used to determine whether the numerical model was describing the actual flow pattern over the corrugation and whether it was predicting convective heat loss accurately. Convective heat loss measurements were taken on a sample of transpired corrugated plate at the corrugation crest using hot-wire anemometry. The experimental results were compared to numerical simulations which used the experimental parameters as inputs. Agreement was found to be good for the numerical model's ability to predict both the general flow pattern and the convective heat loss.

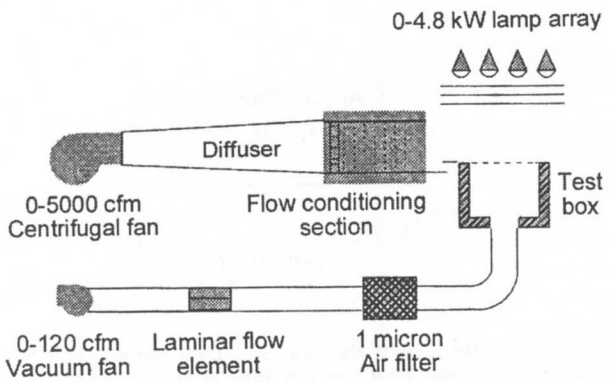

Fig. 3 Experimental facility at NREL (from Kutscher [5])

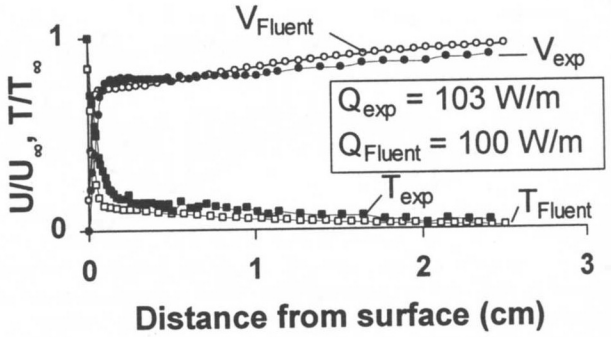

Fig. 4 Experimental and numerical boundary layer profiles for a separated flow case at 0.06 m/s suction air speed and 4 m/s crosswind air speed

The velocity and thermal boundary layers were measured using a TSI hot-wire anemometry system. The temperature profiles were measured using a single-axis probe as a resistance thermometer and velocity profiles by using the system in the conventional manner. The heat loss value was obtained by integrating the velocity and temperature boundary layers on the last downstream crest of the corrugated collector test plate. Profiles of the boundary layers were taken along a crest, also, to determine if the homogenous suction of the model predicted heat loss for a plate with discrete suction. It was found that there was little variation of heat loss along the crest. The experimental uncertainty of the heat loss measurement was determined to be $\pm 4\%$, and qualification tests were performed to compare the heat loss results from this method to those from the measurement of the overall heat balance on the plate. Those tests showed that this technique was measuring heat losses in agreement with the heat balance calculation.

The experimental facility is described in Kutscher [5] and was modified little for this project. Figure 3 depicts the major components. The facility consists of a wind tunnel, a test plate mounting and suction system, and a lamp array. The wind tunnel is an open loop system with the test plate mounted in the exhaust jet. It is capable of providing wind speeds of up to 10 m/s at low turbulence intensities. The test plate is mounted on an insulated, airtight wooden box. Because the plate is mounted within the jet, the length and height of the test plate are limited by the size of the inviscid core of the jet and the flux field of the lamp array. The maximum test plate dimensions are 0.3-m wide by 0.5-m long. Suction velocities are able to exceed 0.1 m/s, depending on the porosity of the plate, but 0.1 m/s is considered the upper limit of suction velocity for typical applications. The lamp array consists of sixteen 300-W floodlamps arranged in a computer-designed pattern to provide illumination of the test plate to within $\pm 2\%$ uniformity. The lamp array voltage is controlled by a pair of variable transformers and can provide a flux of up to 1000 W/m^2.

Comparisons with Numerical Simulations. The test conditions used for the experimental runs were provided as inputs to the numerical model to determine if the simulations could model heat loss accurately. A traverse of a separated flow case at 4 m/s crosswind speed and 0.06 m/s suction air speed is shown in Fig. 4, along with the results from the model, which used as inputs the experimental results for ambient and plate temperatures, air density, crosswind speed, and suction velocity. There is excellent agreement between the model result for convective heat loss, 100 W/m, and the experimental result, 103 W/m. There is also good agreement in the general shapes of the profiles between the experimental and numerical methods.

Another simulation was made at 2 m/s crosswind speed and 0.03 m/s suction air speed. The numerical result delivered a heat loss of 81 W/m, and the experimental result was 83 W/m. The difference between the two methods was less than 3%.

A simulation was also performed on the 0.03 m/s suction air speed and 4 m/s crosswind speed test described above. The model result was 290 W/m, which disagrees with the 137 W/m result in the laboratory. Based on observations of the behavior of the flow over the plate, the asymptotic boundary layer was barely established on the last peak at 0.03 m/s suction air speed and 2 m/s crosswind speed. Hence, one would not expect the last crest at 4 m/s to be in an asymptotic region, thus giving rise to the difference found above. The numerical model was therefore needed to determine results for conditions falling outside the experimental domain.

Summary of the Qualification Tests. Because of the good agreement between numerical and experimental results, and the limitations of the apparatus in terms of plate size that could be tested and the amount of suction air flow it could provide, it was determined that the simulations would be used to develop the correlation of heat loss over the corrugated plate. Much of the experimental domain in which the test section was too short to establish asymptotic conditions was at low suction velocities. This may become an important regime, however, as future solar collector applications may emphasize low suction velocities to increase the temperature rise of the process air [11]. Using computational fluid dynamics allowed the study of a large range of suctions and crosswind speeds that could not be tested in the laboratory, in addition to different plate shapes.

Results and Discussion

Attached Flow. Heat loss in the attached flow case is related to the heat loss for the flat plate [5] by the aspect ratio. The heat losses for the low aspect ratio plate are significantly greater than the equivalent heat losses for a flat plate, using the same projected areas. For the low aspect ratio plate at 0.09 m/s suction air speed, 2 m/s crosswind speed, and 20°C temperature difference, the convective heat loss was 46% greater than that from a flat plate under the same conditions. For the medium aspect ratio plate under the same conditions, convective heat loss was 77% greater than the flat plate result.

For attached flow the following relationships were observed. The asymptotic boundary layer thickness is a function of suction only and not freestream velocity, as in the flat plate case. When plate geometry changes, the greater the aspect ratio, the greater the acceleration over the crest, and the higher the peak velocity in the boundary layer.

The temperature profiles for the flat and corrugated cases are similar, unlike the velocity profiles. The velocity boundary layer at the crest shows an extensive region with velocities greater than free stream, because of the acceleration of the flow over the crest. This is shown in Fig. 5 for one of the runs where velocity and temperature are non-dimensionalized with respect to free stream values. For the low aspect ratio plate, the non-dimensional veloc-

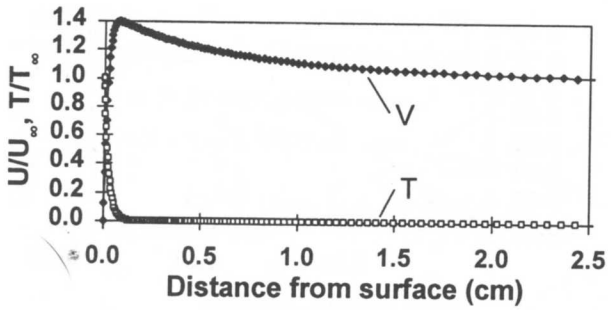

Fig. 5 Numerical results for attached flow boundary layer profiles for the medium aspect ratio plate with 0.09 m/s suction air speed and 2 m/s crosswind air speed

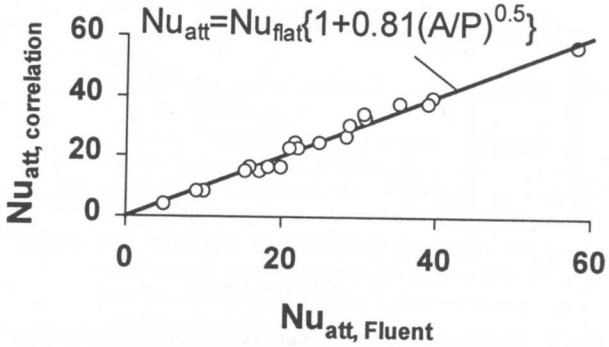

Fig. 6 Correlation of numerical results for attached flow

ity reached a maximum of about 1.25. Because of the large velocities in the boundary later, the integrated heat loss for this geometry was greater than the case of the flat plate. The peak non-dimensional velocity was approximately 1.4 for the medium aspect ratio plate, whose aspect ratio was twice that of the low aspect ratio case. The integrated heat loss for this geometry was 16% greater than the heat loss for a low aspect ratio plate under similar conditions.

The numerical results from the attached flow case were correlated by using the relation for flat plate heat loss and the aspect ratio. The relationship for flat plate heat loss [5] is:

$$Q_{flat}=\frac{\rho c_p \Delta T U_\infty}{V_0}\left[\frac{\upsilon}{\mathrm{Pr}+\mathrm{Pr}^2}\right] \tag{1}$$

The heat loss for attached flow over corrugated plates can be related to that for flat plates by

$$Q_{att}=Q_{flat}\left[1+0.81\left(\frac{A}{P}\right)^{0.5}\right] \tag{2}$$

in which the leading coefficient on the aspect ratio has a coefficient of variation of 7% and the correlation coefficient is 0.98. Since this is laminar flow, and since Q, in the form of a Nu number, can be correlated as a function of Re numbers that use A and P as characteristic dimensions, as shown below, the exponent was fixed at 0.5. Regressions that allowed the exponent to float resulted in an exponent value of 0.51, with coefficients of variation of 44% for the leading coefficient on aspect ratio and 42% on the exponent. It should be noted that the relationship for Q_{flat} was derived analytically and is valid for any Prandtl number, but the experimental correlation for Q_{att} is only valid for air.

The heat losses can be expressed in terms of Nusselt numbers, developed in the following way. The Nusselt number is based on the heat transfer coefficient from the plate to the crosswind during the portion of the plate that consists of the developing region of the periodic boundary layer. The relevant length scale is the starting length required to fully develop the asymptotic boundary layers. The total heat transfer from the plate to the crosswind during the starting length is equal to the convective heat loss from the downstream edge of the plate. Thus,

$$h=\frac{Q_{start}}{A_s \Delta T} \tag{3}$$

where

$$A_s=WL_s \tag{4}$$

and where W is the unit width of the plate and L_s is the starting length. Therefore,

$$\mathrm{Nu}=\frac{Q_{start}}{Wk\Delta T} \tag{5}$$

Thus, the correlation takes the form of

$$\mathrm{Nu}_{att}=\mathrm{Nu}_{flat}\left[1+0.81\left(\frac{A}{P}\right)^{0.5}\right] \tag{6}$$

The correlation fit is shown in Fig. 6 where the x-axis values are actual Nu_{att} obtained from the numerical model and the y-axis values are Nu_{att} predicted by Eq. (6). The ratio of A and P can be replaced by a ratio of Reynolds numbers based on crosswind speed and these characteristic dimensions with no change to the leading coefficient or exponent of the ratio.

Separated Flow. Given a corrugation aspect ratio, for certain combinations of high crosswind speed and low suction velocity, the flow over the corrugations separates and reattaches. With crosswind speed and suction velocity constant, increasing the aspect ratio promotes flow separation. Most of the simulations of the base case plate and all of the simulations of the high aspect ratio plate showed separated flow. The boundary layer separated downstream of the upstream crest and reattached on the upwind facing flank. The points of separation and reattachment were functions of the suction and crosswind speeds. Heat losses were much higher for the separated flow cases than for the attached flow cases for the same values of crosswind speed, suction velocity, and temperature difference.

When wind speed is high, a reduction in suction increases the size of the boundary layers and delays the point of reattachment on the upstream flank of the trough. At a given suction, the effect on the boundary layers with increase in wind speed is to thicken the boundary layers, delay the separation point, and increase the heat loss.

For separated air flow, a correlation of the form

$$\mathrm{Nu}_{sep}=a\,\mathrm{Re}^b\,\Pi^c \tag{7}$$

was sought where Π is a dimensionless group of geometrical parameters. Nu is defined in the same way as for attached flow (Eq. (5)). The Reynolds number is developed as follows. Re is based on suction velocity and starting length:

$$\mathrm{Re}=\frac{V_0 L_s}{\upsilon} \tag{8}$$

From the work on flat plates [5],

$$L_s=\frac{\upsilon U_\infty}{V_0^2} \tag{9}$$

Substituting Eq. (9) into Eq. (8) yields

$$\mathrm{Re}=\frac{U_\infty}{V_0} \tag{10}$$

This is often called the *suction parameter* in the literature, but we can see that with starting length as the appropriate length scale, this velocity ratio represents a Reynolds number.

The appropriate dimensionless group, Π, is the aspect ratio,

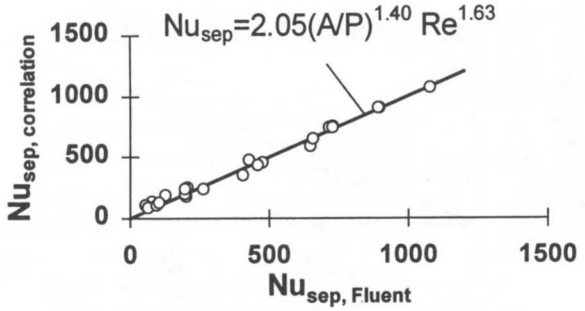

Fig. 7 Correlation of numerical results for separated flow

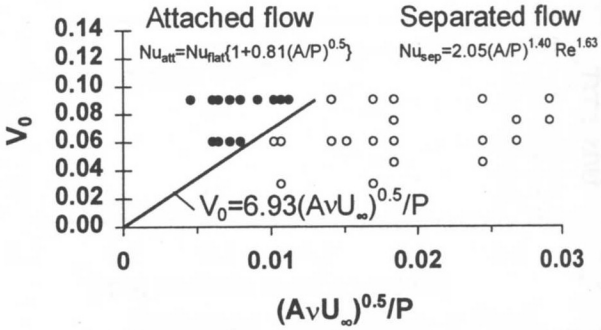

Fig. 8 Numerical data points for attached and separated flow cases and plot of correlation for predicting flow separation

$$\Pi \equiv \frac{A}{P} \tag{11}$$

Correlation of the numerical results then yields

$$\mathrm{Nu}_{sep} = 2.05\left(\frac{A}{P}\right)^{1.40} \mathrm{Re}^{1.63} \tag{12}$$

where the coefficients of variation are 16% for the leading coefficient, 5% for the exponent on aspect ratio, and 3% for the exponent on Reynolds number. The correlation coefficient is 0.99. This fit is displayed in Fig. 7, where on the x-axis are the numerical Nu_{sep} values and on the y-axis are the predicted values using Eq. (12). Since the heat transfer from the plate to the crosswind in the starting length is equal to the convective heat loss at the downstream edge of the plate, use Eq. (5) to calculate heat loss from the Nu_{sep} obtained from Eq. (12).

Suction Required to Prevent Separation. We have presented two correlations for convective heat loss, Eqs. (6) and (12) one for each of the two flow regimes. In order to know which correlation to use, it was necessary to develop a means of determining when the flow over the corrugated plate is attached or separated.

Schlichting [1] showed that the minimum suction required to prevent separation from an arbitrary body shape has the following functional relationship:

$$V_{0_{\min}} \propto \sqrt{\nu\left(\frac{du}{dx}\right)_{\max}} \tag{13}$$

where $u(x)$ is the velocity at the surface in potential flow with no suction. The minimum suction required is a function of the rate of change of velocity near the object with respect to the distance along the object. In a region of adverse pressure gradient, i.e., where the fluid is slowing with increase in x along the object, the suction required to prevent separation increases with greater rate of change of velocity.

In order to apply this relationship, we must find $(du/dx)_{\max}$, the derivative of the potential flow velocity at the surface without suction. Ho and Gelhar [12] presented an analysis of the potential flow over a permeable sinusoidally-shaped plate that can be used to determine $(du/dx)_{\max}$. Consider their analysis in the limit of a very low permeability plate to obtain the variation of u, at the plate surface, in the x direction in potential flow. In the limit of no permeability, the velocity potential function at the surface is simply

$$\phi = -U_\infty A \cos\left(\frac{2\pi x}{P}\right) \tag{14}$$

Local velocity, $u(x)$, is then

$$u(x) = \frac{d\phi}{dx} = U_\infty A\left(\frac{2\pi}{P}\right)\sin\left(\frac{2\pi x}{P}\right) \tag{15}$$

and

$$\frac{du(x)}{dx} = U_\infty A\left(\frac{2\pi}{P}\right)^2 \cos\left(\frac{2\pi x}{P}\right) \tag{16}$$

Thus, the maximum rate of change of the velocity near the wall with respect to distance along the wall varies as

$$\left.\frac{du(x)}{dx}\right|_{\max} \propto \frac{U_\infty A}{P^2} \tag{17}$$

Combining (13) and (17) yields,

$$V_{0_{\min}} \propto \frac{1}{P}\sqrt{A\nu U_\infty} \tag{18}$$

or, expressed as an equality,

$$V_{0_{\min}} = \frac{c}{P}\sqrt{A\nu U_\infty} \tag{19}$$

where c is an unknown constant of proportionality. In order to determine c, we conducted numerical simulations on the low aspect ratio and base case geometries. A value of $c = 6.93 \pm 8.6\%$ was found to predict correctly the flow regime for all of the modeled plates. Thus,

$$V_{0_{\min}} = \frac{6.93}{P}\sqrt{A\nu U_\infty} \tag{20}$$

This relationship is shown in Fig. 8, in which are mapped all of the numerical results, separated and attached. In this plot, the two flow regimes are seen to be clearly delineated by the relationship in Eq. (20), and the heat transfer correlations for the two regimes are shown as well. The relationship in Eq. (20) can also be put in dimensionless form, with Reynolds numbers based on suction velocity and pitch, and crosswind speed and amplitude. Thus, the correlation for flow attachment is

$$\mathrm{Re}_{V_0,P} \geq 6.93\,\mathrm{Re}_{U_\infty,A}^{0.5} \tag{21}$$

For cases in which the condition in Eq. (21) is met, the attached flow correlation, Eq. (6), should be used to determine heat loss to the crosswind. For cases in which the condition for attachment is not met, the separated flow correlation, Eq. (12), should be used.

The separated flow crosswind heat loss from corrugated plates is much higher than that from flat plates. For example, at a suction velocity of 0.03 m/s and a crosswind speed of 5 m/s, heat loss from a base case corrugated collector 3.2 m long on each side is 30% of the incident solar radiation. For a flat plate under identical conditions, the heat loss is approximately 3%. However, heat loss as a fraction of total incident radiation drops as collector size increases, making this an issue primarily for small installations. Figure 9 shows how the convective heat loss varies with crosswind speed for the medium aspect ratio plate at a suction of 0.06

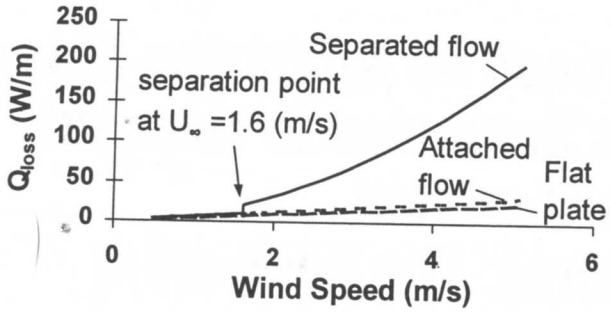

Fig. 9 Increase in heat loss when separation occurs for a typical case

m/s. At low wind speeds, the flow is attached and the wind heat loss is low. When the wind speed is high enough to cause separation, the wind heat loss increases significantly.

Conclusion

Wind tunnel experiments showed that a numerical model of flow over a sinusoidally corrugated plate with uniform suction accurately represented the case of discrete holes. Correlations for heat loss from the plate to the crosswind were developed for both the attached and separated flow cases, and a criterion for attached flow was developed. In summary, the flow is attached if

$$\mathrm{Re}_{V_0,P} \geq 6.93\,\mathrm{Re}_{U_\infty,A}^{0.5} \tag{21}$$

For convective heat loss, if the flow is attached, use

$$\mathrm{Nu}_{att} = \mathrm{Nu}_{flat}\left[1 + 0.81\left(\frac{A}{P}\right)^{0.5}\right] \tag{6}$$

If the flow is separated, use

$$\mathrm{Nu}_{sep} = 2.05\left(\frac{A}{P}\right)^{1.40}\mathrm{Re}^{1.63} \tag{12}$$

These results are immediately applicable to the determination of the wind heat loss from corrugated transpired solar collectors operated at low suction velocities.

Nomenclature

A = amplitude of corrugations, in., m
A_s = area of corrugated plate during starting length, m^2
c = dimensionless constant of proportionality used in Eq. (19)
c_p = specific heat of air, J/kg-K
h = heat transfer coefficient, W/m^2-K
k = thermal conductivity, W/m-K
L_s = starting length, corrugated plate, m
Nu = Nusselt number, corrugated plate, $Q_{start}/(Wk\Delta T)$
Nu_{att} = Nusselt number for corrugated plates in attached flow, $Q_{att}/(Wk\Delta T)$
Nu_{flat} = Nusselt number for flat plates, $Q_{flat}/(Wk\Delta T)$
Nu_{sep} = Nusselt number for corrugated plates in separated flow, $2.05(A/P)^{1.40}\,\mathrm{Re}^{1.63}$
P = wavelength of corrugations, m
Pr = Prandtl number, ν/α
Q_{att} = convective heat loss from corrugated plate in attached flow, per unit downstream width of plate, W/m, $Q_{flat}[1+0.81(A/P)^{0.5}]$
Q_{exp} = experimental heat loss per unit width shown in Fig. 4, W/m
Q_{flat} = convective heat loss from flat plate, per unit downstream width of plate, W/m, $(\rho c_p \Delta T U_\infty / V_0)[\nu/(\mathrm{Pr}+\mathrm{Pr}^2)]$
Q_{Fluent} = numerical heat loss per unit width shown in Fig. 4, W/m
Q_{del} = heat transfer to the suction air stream per unit width of plate, W/m
Q_{loss} = convective heat loss from corrugated plate per unit width of plate, W/m, numerically equal to Q_s
$Q_{rad,net}$ = net radiant heat transfer to the plate per unit width of plate, W/m
Q_s = heat transfer from corrugated plate surface to crosswind during starting length, per unit width, W/m
Q_{start} = heat transfer from corrugated plate surface to crosswind during starting length, W
Re = Reynolds number, corrugated plate, U_∞/V_0
$\mathrm{Re}_{V0,P}$ = Reynolds number based on suction velocity and pitch, $V_0 P/\nu$
$\mathrm{Re}_{U\infty,A}$ = Reynolds number based on free stream velocity and amplitude, $U_\infty A/\nu$
T = temperature normalized with respect to free stream temperature
$T_{\exp}$ = experimental temperature normalized with respect to free stream temperature
T_{Fluent} = numerical temperature normalized with respect to free stream temperature
ΔT = temperature difference between surface of corrugated plate and the free stream, K
u = local velocity in boundary layer parallel to plate, m/s
U_∞ = free stream velocity, m/s
V = velocity normalized with respect to free stream velocity
V_0 = average suction face velocity, m/s
$V_{\exp}$ = experimental velocity normalized with respect to free stream velocity
V_{Fluent} = numerical velocity normalized with respect to free stream velocity
W = width of test plate, m
x = distance along plate, m

Greek

α = thermal diffusivity, m^2/s
δ_{99} = point in boundary layer where air velocity is 99% of free stream
ν = kinematic viscosity of air, m^2/s
Π = dimensionless group, A/P
ρ = air density, kg/m^3
ϕ = velocity potential function, m^2/s

References

[1] Schlichting, H., 1979, *Boundary Layer Theory*, Seventh Edition, McGraw-Hill Book Co., New York, pp. 392–393.
[2] Iglisch, R., 1944, "Exact Calculation of Laminar Boundary Layer in Longitudinal Flow Over a Flat Plate with Homogeneous Suction," Tech. Memo. No. 1205, National Advisory Committee for Aeronautics, Washington, D.C.
[3] Maddaeus, A. D., and Shanebrook, J. R., 1983, "The Three-Dimensional Laminar Asymptotic Boundary Layer with Suction," J. Eng. Math., **17**, pp. 73–91.
[4] Arpaci, V. S., and Larsen, P. S., 1984, *Convection Heat Transfer*, Prentice-Hall, Englewood Cliffs, NJ, pp. 160–169.
[5] Kutscher, C. F., 1992, "An Investigation of Heat Transfer for Air Flow Through Low Porosity Perforated Plates," Ph.D. thesis, Univ. of Colorado, Dept. of Mech. Eng.
[6] Kutscher, C. F., Christensen, C. B., and Barker, G. M., 1993, "Unglazed Transpired Solar Collectors: Heat Loss Theory," ASME J. Sol. Energy Eng., **115**, pp. 182–188.
[7] Bordner, Gary L., 1978, "Nonlinear Analysis of Laminar Boundary Layer Flow Over a Periodic Wavy Surface," Phys. Fluids, **21**, pp. 1471–1474.
[8] Bordner, Gary L., 1980, "Nonlinear Analysis of Laminar Boundary Layer Flow Over a Periodic Wavy Surface—Part II: Long Waves," Phys. Fluids, **23**, pp. 858–863.
[9] Patankar, S. V., 1980, *Numerical Heat Transfer and Fluid Flow*, Hemisphere Publishing Corp., New York.
[10] Conserval Engineering, Inc., Toronto, Canada.
[11] Hollick, J., 1994, private communication, Conserval Engineering, Inc., Toronto.
[12] Ho, R. T., and Gelhar, L. W., 1973, "Turbulent Flow with Wavy Permeable Boundaries," J. Fluid Mech., **58**, Pt 2, pp. 403–414.